Nuclear Instruments and Methods in Physics Research A 478 (2002) 440–443

NUCLEAR INSTRUMENTS & METHODS IN PHYSICS RESEARCH Section A

www.elsevier.com/locate/nima

Timing characteristics of scintillator bars

S. Denisov[a], A. Dzierba[b], R. Heinz[b], A. Klimenko[a], V. Samoylenko[a,*], E. Scott[b], A. Shchukin[a], P. Smith[b], C. Steffen[b], S. Teige[b]

[a] *Institute for High Energy Physics, State Comm. for Util. of Atom Energy, Protvino 142284, Moscow Region, Russia*
[b] *Physics Department, Indiana University, Bloomington, IN 47405, USA*

Abstract

The proposed Hall D detector at Jefferson Lab will have a time-of-flight detector composed of long and narrow scintillator bars. We have evaluated the time resolution of two bar prototypes in particle beams at the Institute for High Energy Physics in Protvino, Russia. The bars are 2.0 m long and have square cross-sections of size 2.5 and 5.0 cm^2. In this paper, we present results on how the time resolution of each of these bars depends on the entry position of the beam into the scintillator, on the material used for scintillator wrapping and on the phototube used for the readout.

PACS: 29.40.Mc

Keywords: Hall D; Time of flight; Particle identification

1. Introduction

The proposed Hall D [1] project at Jefferson Lab in Virginia will use a hermetic detector to search for photoproduced mesons which carry quantum numbers (J^{PC}) that are exotic, i.e. cannot be formed from a simple $q\bar{q}$ combination. The detector is optimized for incident photon energies from 8 to 10 GeV. In order to carry out the spin analysis needed to identify exotic quantum numbers, all charged particles in an event, including the decay products of mesons, must be momentum analyzed and identified as π, K or proton (p). This identification will be carried out using an atmospheric gas (C_4F_{10}) Cherenkov counter and a time-of-flight (TOF) wall. The latter will consist of two orthogonal planes of scintillator bars. The bars will be 2 m long with square transverse cross-sections of dimension yet to be determined. The width will be between 2.5 and 5.0 cm. The timing resolution must be less than 100 ps. In this paper, we report on measurements of time resolution as a function of the scintillator wrapping and type of phototube performed at IHEP for two 2 m long scintillator bars of different transverse dimensions.

2. Experimental arrangement

The layout of the apparatus is shown in Fig. 1. The two bars that were tested were 2 m long and had square cross-sections of size 2.5 and 5.0 cm^2. The scintillator is type EJ-200, purchased from the Eljen Corporation [2]. This scintillator has a decay time of 2.1 ns, a bulk attenuation length of 4 m, an

*Corresponding author.
E-mail address: samoylenko@mx.ihep.su (V. Samoylenko).

0168-9002/02/$ - see front matter
PII: S 0 1 6 8 - 9 0 0 2 (0 1) 0 1 7 9 8 - 3

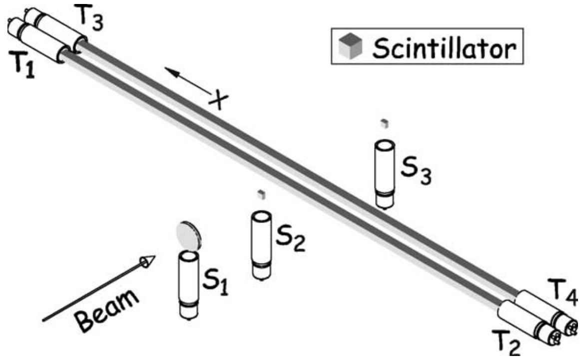

Fig. 1. Experimental setup for TOF measurements.

index of refraction of 1.58, and a peak in the emission spectrum at 425 nm. The surfaces of two of the four long sides of each bar were in contact with the casting form and had no other preparation. The other two long sides and the two ends of each bar were diamond fly-cut in order to minimize losses due to surface imperfections. A phototube was placed on each end of each bar. The two bars, with their phototubes, were placed in a light-tight box. The bars were either bare or wrapped, and a partition inside the light-tight box prevented optical cross talk between the bars.

We define x as the position of the center of the long scintillator relative to the beam. We operated at a maximum beam intensity of 5×10^5 particles per 1-s spill. The beam defining counters shown in Fig. 1 are S_1, S_2, and S_3. The cross-sectional size of the beam was large compared to the 2 cm × 2 cm size of S_2 and S_3. S_2 and S_3 were each 1.25 cm thick and both coupled to an XP2020 phototube with a 5 cm air gap. S_1 was not used for timing purposes or to define the effective size of the beam. All phototube signals went into a constant fraction discriminator, eliminating the need for any time walk corrections.

Before showing our results in Section 4, we present in Section 3 some general characteristics of the 2.5 cm bar, wrapped in aluminum foil and attached to T_1 and T_2 with optical grease. In Section 3, the data were obtained using a 4.3 GeV/c unseparated positive secondary beam.

3. ADC and TDC results

In Fig. 2, we show how the log of the ADC value corresponding to the peak position of the pulse height distribution (as determined from a Moyal [3] fit) depends on the beam entry position along the x-axis. The ADC data deviate noticeably from an exponential dependence on x. However, a Monte Carlo investigation shows that the shape of the data is consistent with a model of photon propagation in which there is a bulk attenuation of 4 m and a loss per surface reflection of ~1%.

The average T_1 TDC time versus x is plotted in Fig. 3. The slope of this line leads to an effective speed of light along the x-axis of 15.6 cm/ns. Using the index of refraction of the scintillator, we conclude that the average angle of the light with respect to the x-axis is 35°.

Fig. 4 shows the time resolution, $\sigma(T_{av})$, versus x, where open circles are for the 5.0 cm bar and closed triangles are for the 2.5 cm bar. We calculate the average time, T_{av} and its resolution as follows. Specifically,

$$T_{av} = \frac{T_1\sigma^2(T_2) + T_2\sigma^2(T_1)}{\sigma^2(T_1) + \sigma^2(T_2)} \quad (1)$$

where T_1 represents the time of the pulse from T_1 (corrected for travel time along the bar) and $\sigma(T_1)$ is the time resolution of T_1. From Eq. (1), we can calculate the time resolution of T_{av}, $\sigma(T_{av})$, from

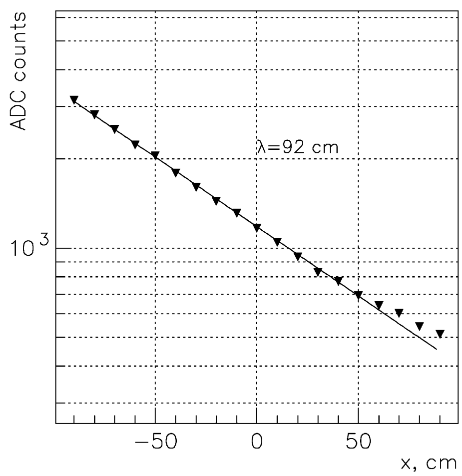

Fig. 2. Average ADC versus x position.

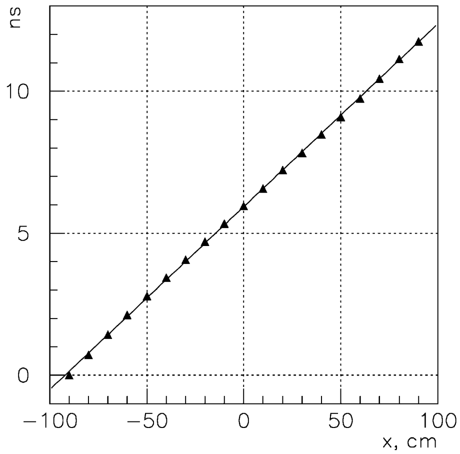

Fig. 3. The average T_1 TDC time versus x.

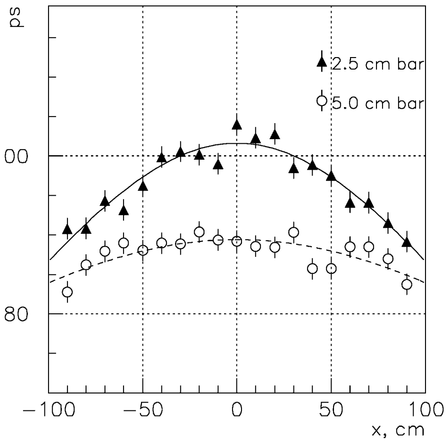

Fig. 4. $\sigma(T_{av})$ time resolution versus x.

that of T_1 and T_2:

$$\frac{1}{\sigma^2(T_{av})} = \frac{1}{\sigma^2(T_1)} + \frac{1}{\sigma^2(T_2)} \quad (2)$$

where $\sigma(T_1)$ and $\sigma(T_2)$ are corrected for an 80 ps common start time resolution.

We note that the time resolution is worse when the beam goes through the center of the bar ($x = 0$) because there is less total light. Also, the time resolution in the center is poorer for the 2.5 cm bar (101 ps) than for the 5.0 cm bar (87 ps). These time resolutions do not include corrections for the finite size of the trigger counters, an effect that reduces the resolution by $\sim 10\%$.

Table 1
Attenuation length and time resolution for the 2.5 and 5.0 cm bars with different wrappings. The error on quoted time resolutions in all cases is 2 ps

	Attenuation length (cm)	Time resolution in center of bar (ps)	Time resolution 10 cm from bar end (ps)
2.5 cm bar			
Bare	141 ± 14	102	81
Aluminum foil	143 ± 14	101	79
Tyvek	134 ± 13	106	91
5.0 cm bar			
Bare	248 ± 25	87	79
Aluminum foil	292 ± 29	87	84
Tyvek	217 ± 22	91	86

4. Dependence on wrapping

We next investigated scintillator wrapping and phototubes in a 40 GeV/c negative beam containing over 98% pions. There was no optical coupling of the phototubes in these studies. Table 1 shows how the light attenuation length and time resolution depend on the three wrapping conditions, bare (no wrapping), aluminum foil (shiny side in) and Tyvek.

A fit of the ADC data to an exponential yields an attenuation length which depends on the number of data points used in the fit, since the data themselves are not exponential in nature. (This is shown for T_1 in Fig. 2.) In Table 1, we show the attenuation length from an exponential fit to the three data points farthest from the phototube, to be used as a figure-of-merit. In Table 1, as in Fig. 3, we correct for the common start time resolution but not for the finite size of the trigger counters.

We conclude from Table 1 that the 5.0 cm bar has a smaller attenuation length than the 2.5 cm bar, with a typical effective attenuation length of about 250 cm versus 140 cm. (The errors on the attenuation length are estimated, largely from comparing the redundant results coming from the two phototubes.) There is no large variation between the three wrapping states, though there is an indication that Tyvek has the poorest (smallest) attenuation length.

As is the case for the attenuation length, the time resolution in the center of the bar and at the bar end suggest that Tyvek wrapping has a somewhat inferior time resolution, a result consistent with a smaller signal due to a larger light loss. The time resolution for the larger bar is definitely superior to that of the smaller bar (presumably because the 5.0 cm bar produces twice the light, and less of its light is lost due to a reduced number of surface reflections).

Table 2
Time resolution for various phototubes

Phototube	Time resolution (ps)
2.5 cm bar	
XP2020	101
FEU 115	172
Hamamatsu R5506	167
Hamamatsu R5946	102
5.0 cm bar	
XP2020	87
XP2020/UR	82

5. Studies of phototubes

We used five different phototubes for the bar readout. In the first comparison, we sequentially placed four of them on the 2.5 cm bar that was wrapped with aluminum foil and sent the beam through the center of the bar. The top of Table 2 shows the time resolution, $\sigma(T_{\text{av}})$, for each of the four tubes.

Next, we compared an XP2020/UR to an XP2020 using the 5.0 cm bar wrapped in aluminum foil. The results are in the bottom section of Table 2. We conclude that the time resolutions of the Hamamatsu R5946 and the XP2020 are about the same, and much better than the FEU 115 and the Hamamatsu R5506. Also the XP2020/UR has a slightly better resolution than the XP2020.

6. Conclusion

We have presented the x-dependence of the time resolution, and other general amplitude and timing features, for two scintillator bars placed in a 4.3 GeV/c positive secondary beam at IHEP. Using a 40 GeV/c negative beam, we have shown how the time resolution of the two scintillator bars depends on the scintillator wrapping and on the phototubes used. The bar sizes were chosen to be appropriate for the Hall D experiment planned for Jlab.

Acknowledgements

We appreciate financial support from the US Department of Energy and the Russian RFBR (grant 00-15-96733), and valuable contributions from I. Polezhaeva, A. Godov, A. Romadanov, I. Beljakov, S. Zvjagintsev, I. Shvabovich and A. Soloviev.

References

[1] A. Dzierba, C. Meyer, E. Swanson, Am. Sci. 88 (2000) 446; A. Dzierba, N. Isgur, CERN Courier 40 (2000) 23. See also http://dustbunny.physics.indiana.edu/HallD/.
[2] http://www.apace-science.com/eljen/.
[3] J. Moyal, Philos. Mag. 46 (1955) 263.